Interpretation Method of GATEM Data based on PID Controller Iteration Downward Continuation Method

Shanshan Guan [1], Bingxuan Du [1], Dongsheng Li [1], Yuan Wang [1], Yu Zhu [1], Qiong Wu [1*], and Yanju Ji [1,2]

[1] Department of Instrumentation and Electrical Engineering
Jilin University, Changchun 130026, China

[2] Key Laboratory of Earth Information Detection Instrumentation of Ministry of Education,
Jilin University, Changchun 130026, China
guanshanshan@jlu.edu.cn, dubx20@mails.jlu.edu.cn, lidongsheng86@sina.cn, wangyuan_ciee@jlu.edu.cn,
zhuyu@jlu.edu.cn, wuqiong_515@sina.cn*, jiyj@jlu.edu.cn

Abstract ─ The Ground-source Airborne Time-domain Electromagnetic (GATEM) system has advantages for high efficiency and complex areas such as mountainous zone. Because of ignoring the impact of flight height, the section interpretation method seriously affects the interpretation and imaging accuracy of shallow anomalies. The PID controller iteration downward continuation method is proposed. Based on the original iteration continuation method, the differential coefficient and integral coefficient are added. The result shows that the new method remarkably decreases the iteration number, and the accuracy are verified by comparison with the numerical integration solution. The PID controller iteration downward continuation method is applied to the interpretation of GATEM data. For synthetic data, the interpretation results of continued electromagnetic response are closer to the true model than the z = 30 m interpretation results. The method is also applied to GATEM field data in Yangquan City, Shanxi Province, China. The interpretation results perform reliability using PID controller iteration downward continuation method in a GATEM field.

Index Terms ─GATEM system, interpretation, PID controller iteration downward continuation method.

I. INTRODUCTION

The Ground-source Airborne Time-domain Electromagnetic (GATEM) system contains a long grounded electric source as the transmitter unit, and the portable receiving device, which is mounted on the platform of aircraft. The GATEM system can realize efficient and fast geological survey tasks in complex areas, such as beach, volcanic geological structure, and seawater intrusion structure [1-4]. It has the advantages of large exploration depth, low flight cost, and high security comparing with those of the airborne time-domain electromagnetic system. In recent years, it has gradually become a research hotspot of the time-domain electromagnetic system.

To recognize electrical resistivity anomaly, data procession is necessary for the GATEM field data. Scholars have carried out many studies on it. Sasaki et al. [5] realize a three-dimensional inversion for grounded electrical source airborne transient electromagnetic (GREATEM) based on the least square method. This method is verified by a theoretical model; however, it is not used in field data interpretation. Allah et al. [6] apply a three-dimensional numerical simulation method to fit field data by changing related parameters of the model. Although the results are almost the same with geological data, it takes a lot of time. Liang et al. [7] realize an inversion algorithm for GREATEM using the deformed Born iteration method. This method is verified by the theoretical model and applied to the field data. The results are basically consistent with the geological data. Wu et al. [8] realize GATEM modeling and interpretation methods for a rough medium. The interpretation method based on artificial neural networks is applied to the field data, and the results are consistent with the geological data. A section interpretation method (the long wire source is solved by splitting into a large number of electric dipoles [9-10]) is widely used because of its simplicity and high efficiency [1,4,11-12]. However, this method is limited to the high-precision interpretation of ground electromagnetic data. The effect of the flight height on interpretation is ignored during data processing, so the interpreted electrical resistivity is bound to differ from the true electrical resistivity. To avoid the impact of the flight height on interpretation, this paper proposes an interpretation method based on PID controller iteration downward continuation method.

Submitted On: December 18, 2020
Accepted On: May 8, 2021

https://doi.org/10.47037/2020.ACES.J.360602

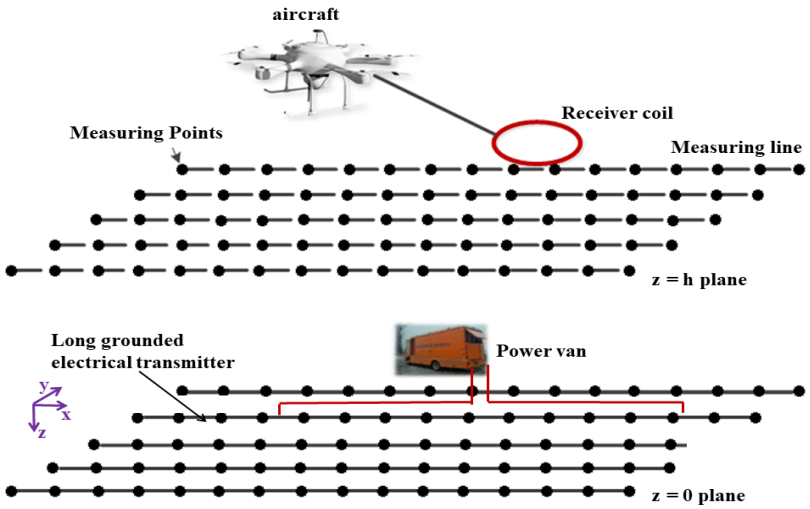

Fig. 1. Configuration of the GAFEM system and schematic diagram of measuring points in a two-dimensional (2D) plane field.

The FFT downward continuation method has an amplification effect on high-frequency noise. To solve the problem, scholars have conducted relevant research in recent years. A stable downward continuation algorithm is presented [13], which is based on the stable vertical derivatives computation obtained by the ISVD method and Taylor series expansion of the potential field. Xu et al. put forward the iteration downward continuation method, which is much better than the FFT [14-15]. At the same time, it does not require solving algebraic equations. Ali et al. [16] present a discrete equivalent source method to perform a stable downward continuation of gravity anomaly. Through automatically selecting an effective amount of the discrete sources, the coefficient matrix size is reduced. The common methods have disadvantages in obtaining optimal results because of divergence and instability. The mean-value theorem for potential field is derived [17]. Compared with the FFT and Taylor series method, the integrated second vertical derivative Taylor series method has very little boundary effect and is still stable in noise. The downward continuation method is also used to the aeromagnetic data [18]. By continuing the field to a level which is a fraction of the distance to the source, it ensures stability by preventing continuation down to or past the source, but its application is restricted to the tilt angle of vertically dipping magnetized contacts. In order to solve the problems, it continues the data to a distance that is a fraction of the current depth, rather than by a fixed distance [19]. The new method is considerably more general in application.

When using the section interpretation method to interpret GATEM data, the accuracy of the shallow anomaly is affected because of ignoring the flight height. In this paper, a PID controller iteration downward continuation method is proposed to improve the interpretation accuracy of the GATEM data. In order to improve the calculation speed, the integral and differential terms are added to the original iteration continuation method, and the PID coefficients k_p, k_d and k_i are studied. Finally, the PID controller iteration downward continuation method is used in simulated data interpretation, and it is also applied in GATEM field data of Yangquan, Shanxi Province, China.

II. METHODS

A. The GATEM response

The GATEM system mainly contains a several-km-long grounded electrical transmitter and an aircraft equipped with an induction coil and a receiver (Fig. 1). The grounded electrical transmitter comprises of high-powered transmitter and a long grounded wire. The transmitter injects a bipolar square wave current +, 0, -, 0 into the ground. The aircraft's operating height might range from 10 m to 500 m and flight speed might be 4 − 20 m⁄s. The vertical component of the induced electromotive force (V_z) due to a step function current in a horizontal layered earth model is expressed as follows [20]:

$$V_z = -i\omega\mu_0 \frac{IS}{4\pi}\int_{-L}^{L}\frac{y}{R}\int_0^{\infty}(1+r_{\mathrm{TE}})e^{u_0 z}\frac{\lambda^2}{u_0}\mathrm{J}_1(\lambda R)d\lambda dx', \quad (1)$$

where I is the transmitter current, S is the area of induction coil, $2L$ is the length of the ground wire, r_{TE} is the reflection coefficient, λ is the Hankel transform integral variable, $u_0 = \lambda$ in the quasistatic electromagnetic field, R is the source-receiver distance $R = \left[(x-x')^2 + y^2\right]^{1/2}$, x' is the integral variable, x is the horizontal longitudinal offset, y is the horizontal

transverse offset, $\omega=2\pi f$ and f is frequency (Hz), μ_0 is the magnetic permeability, and J_1 is the first-order Bessel function. In this case, z is the vertical offset, positive down.

Equation 1 can be calculated by the Hankel transformation algorithm [21], which can be converted from a frequency domain to a time domain by using the Guptasarma digital filtering method [22], then a theoretical induced electromotive force at the $z = 0$ plane is obtained. To verify the correctness of equation 1 calculation, the result is compared with the analytical solution [23]:

$$V_z = -\mu_0 s \frac{\partial H_z}{\partial t} = \frac{2I}{\pi \mu_0 \sigma y^3}\left\{\left(1+\theta^2 y^2\right)e^{-\theta^2 y^2} erf(\theta L) - \frac{L}{R}\left(1+\frac{y^2}{2R^2}\right) erf(\theta R) + \frac{\theta L y^2}{\sqrt{\pi} R^2} e^{-\theta^2 R^2}\right\}, \quad (2)$$

where $R = [y^2 + L^2]^{1/2}$, $\theta = \sqrt{\frac{\mu_0 \sigma}{4t}}$, σ is the electrical conductivity, erf is the error function $erf(x) = \frac{2}{\sqrt{\pi}} \int_0^x e^{-\eta^2} d\eta$.

An example of a homogeneous half-space with 100 Ω·m is calculated. The calculation parameters are as follows: the length of the long grounded electric source is 1 m, the transmitter current I = 10 A, the receiver coil equivalent area S = 1 m^2, and the receiver location coordinates x = 0 m, y = 400 m, z = 0 m. The calculated response is compared with the analytical solution (Equation 2), which is shown in Fig. 2. They coincide with each other.

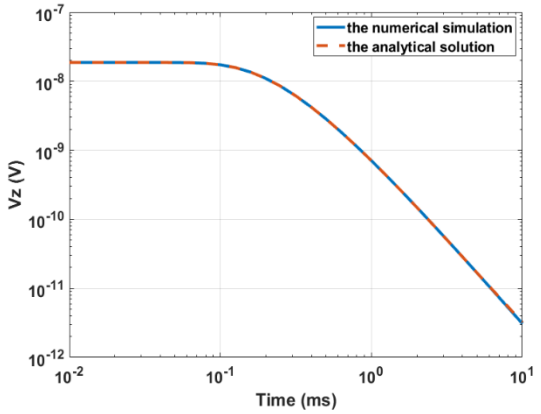

Fig. 2. Comparison of the numerical simulation and analytical solution of the GATEM response in a homogeneous half-space.

A schematic diagram of measuring points in a 2D plane field is shown in Figure 1. The electromagnetic responses at different measuring points are calculated by using the above method of 1D numerical solution method. Then, the theoretical electromagnetic responses of the observation surface $z = h$ and the reference surface $z = 0$ are constructed.

B. The PID controller iteration downward continuation method

1) Downward continuation theory

The GATEM responses usually are interpreted by section interpretation method which is limited to the high-precision interpretation of ground data. Downward continuation of GATEM response is important in the interpretation to improve data interpretation accuracy, because the receiving height of GATEM detection is usually tens of meters above the ground and the section interpretation method might be affected by receiving height. Xu [14] derives the potential field iteration method formula and proposes a downward continuation theory based on the iteration method. Its basic theory is that it transforms unstable downward continuation to stable upward continuation. First, the magnetic fields of $z = 0$ plane assign $z = h$ plane as its initial values. Then, the magnetic fields at the reference surface are upward continued. Finally, the difference between the upward continuation result and the magnetic field at $z = 0$ plane is calculated, which is used to revise the magnetic fields at $z = h$ plane. We repeat the process until precision is satisfied. The original iteration equation is as follows [14]:

$$u^{n+1}(x, y, z = 0) = u^n(x, y, z = 0) + k_p \cdot e_r^{\,n}, \quad (3)$$

where $u^{n+1}(x, y, z = 0)$ is the electromagnetic response after downward-continuation at $z = 0$ plane, k_p is the proportionality factor, n is the number of iterations, $e_r^{\,n} = u^n(x, y, z = h) - f(x, y, z = h)$ is an error term, $u^n(x, y, z = h)$ is the upward continuation electromagnetic response of $u^n(x, y, z = 0)$ at $z = h$ plane, h is the flight height, and $f(x, y, z = h)$ is the measured electromagnetic response at $z = h$ plane.

A large number of data need lot of continuation time, so the iterative process could not be proceeded successfully. In this paper, based on an original downward continuation iteration method, the downward continuation that combines the PID controller theory is proposed. A proportional-integral-differential controller is added. So, original iteration equation 3 can be revised [24]:

$$u^{n+1}(x, y, z = 0) = u^n(x, y, z = 0) + k_p \cdot e_r^{\,n} + k_i \cdot \sum_{i=1}^{n} e_r^{\,i} + k_d \cdot (e_r^{\,n} - e_r^{\,n-1}), \quad (4)$$

where k_i is the integral coefficient, k_d is the differential coefficient, $\sum_{i=1}^{n} e_r^{\,i}$ is the integral term and $e_r^n - e_r^{n-1}$ is

the differentiation term. By adjusting the proportionality factor, differential coefficient, and integral coefficient together, the convergence speed is accelerated.

2) Optimal parameters for the PID controller iteration downward continuation

The proportionality factor, differential coefficient, and integral coefficient can be determined by experience or artificial fish swarms algorithm (AFSA). AFSA can better obtain optimal parameter values. The objective function is defined as:

$$\eta = \max\left\{\frac{u^n(x,y,z=h) - f(x,y,z=h)}{u^n(x,y,z=h)} \times 100\right\}. \quad (5)$$

The process of AFSA is as follows: (1) Artificial fish is initialized. It includes the number of artificial fish, the position of an artificial fish swarm, the maximum try number for foraging behavior, and an accuracy value. The individual position of artificial fish swarm is initialized by chaotic transformation. (2) The food concentration function, quality of individual artificial fish and distance between two artificial fish are calculated. (3) The artificial fish updates itself by foraging, swarming and following. (4) When the value of relative error objective function η is less than preset accuracy, the proportionality factor k_p, differential coefficient k_d, and integral coefficient k_i are obtained.

Figures 3 (a)-(c) show transient process curves that correspond to different PID parameters when t = 0.01 ms. The numbers of iterations are 50000 when parameters of the PID controller iteration are kp = 2, kd = 0.2 and ki = 0.1, 42710 when kp = 3, kd = 0.5 and ki = 0.1, and 31390 when kp = 4, kd = 0.9 and ki = 0.3. Figures 3 (d)-(f) show transient process curves that correspond to different PID parameters when t = 0.25 ms. The numbers of iterations are 4123 when kp = 2, kd = 0.2 and ki = 0.1, 3415 when kp = 3, kd = 0.5 and ki = 0.1, and 2094 when kp = 4, kd = 0.9 and ki = 0.3. Figures 3 (g)-(i) show transient process curves that correspond to different PID parameters when t = 3.16 ms. The number of iterations is 11040 when kp = 2, kd = 0.2 and ki = 0.1, 8872 when kp = 3, kd = 0.5 and ki = 0.1, and 5724 when kp = 3, kd = 0.5 and ki = 0.1. Figure 3 shows that the number of iterations is changing with time. The reason is that absolute errors of electromagnetic responses are varied on the ground and in the air at different times. The number of iterations gets minimal when k_p = 4, k_d = 0.9 and k_i = 0.3.

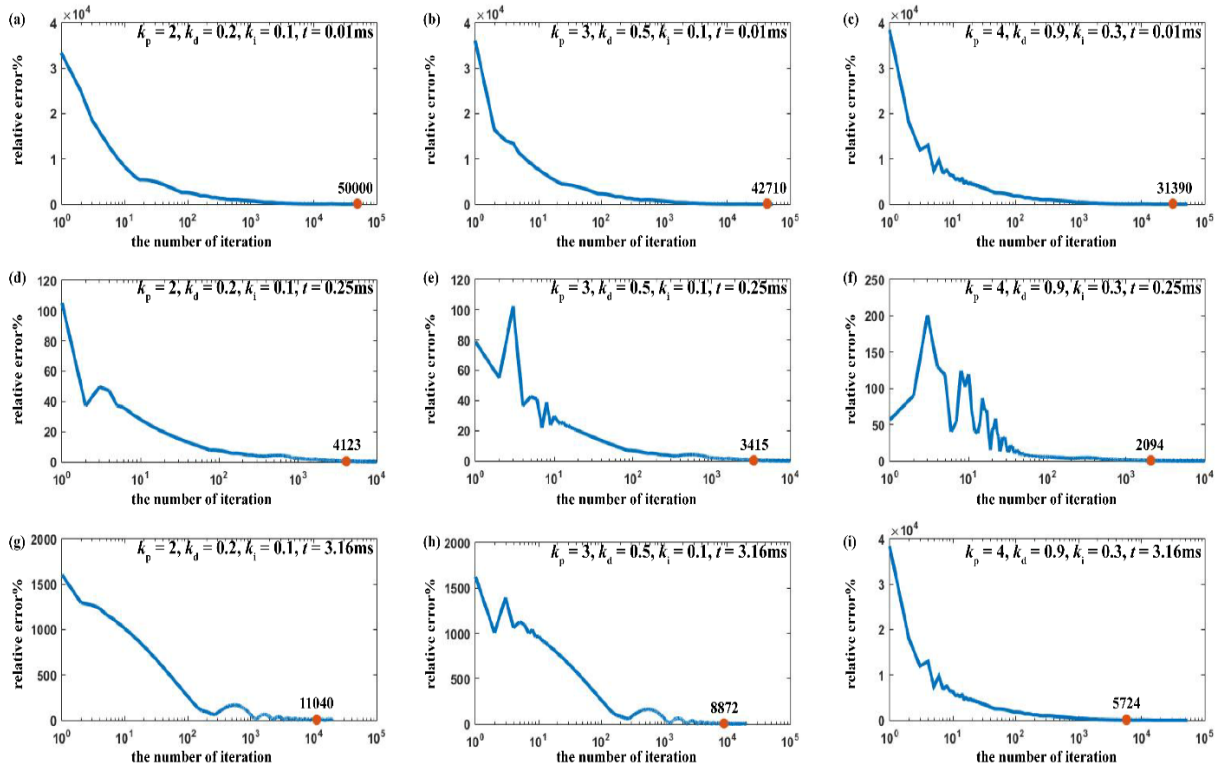

Fig. 3. PID transient process curves. (a)-(c) Transient process curves that correspond to different PID parameters when t = 0.01 ms. The numbers of iterations are 50000, 42710, and 31390 at the orange point. (d)-(f) Transient process curves that correspond to different PID parameters when t = 0.25 ms. The numbers of iterations are 4123, 3415, and 2094 at the orange point. (g)-(i) Transient process curves that correspond to different PID parameters when t = 3.16 ms. The numbers of iterations are 11040, 8872, 5724 at the orange point.

Figure 4 shows the transient process curves based on the original iteration and PID controller iteration when t = 0.05 ms. The optimal proportionality factor of the original iteration is k_p = 2. The parameters of the PID controller iteration are k_p = 4, k_d = 0.9 and k_i = 0.3. The iteration number of an original iteration method is 16210, which is above 5 times PID controller iteration number 3155. In other words, with same accuracy, the PID controller iteration method has less time-consuming. These results indicate that the PID controller iteration downward continuation method is effective and efficient.

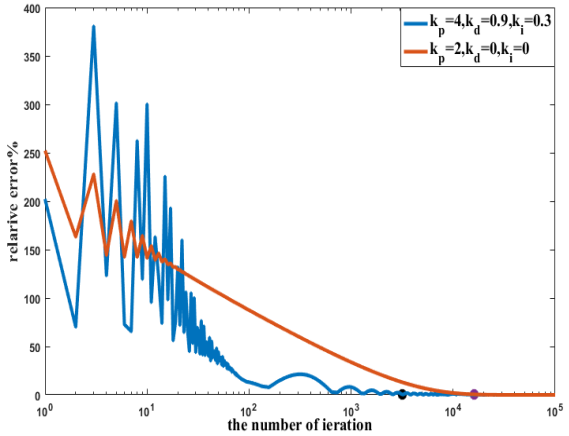

Fig. 4. Transient process curves based on the original downward continuation iteration method and PID controller iteration downward continuation method when t = 0.05 ms.

C. Interpretation methods

The GATEM responses can be interpreted by section interpretation method. The long grounded electric source is solved by splitting into numbers of electric dipoles. The electromagnetic response can be [10]:

$$V_z = \sum_{i=1}^{N} \frac{IS\mu_0 yds}{8\pi t\theta^2 r_i^5}[3erf(\theta r_i) - \frac{2}{\sqrt{\pi}}\theta r_i(3+2\theta^2 r_i^2)e^{-\theta^2 r_i^2}]. \quad (6)$$

where ds is the length of electric dipole, t is the sampling time, $r_i = \sqrt{(x-x_i)^2 + y^2}$. After the value of θ is obtained, the apparent electrical resistivity will be $\rho = \frac{\mu}{4t\theta^2}$. The diffusion depth can be estimated by Spies [25]: $d = \sqrt{\frac{2t\rho}{\mu}}$.

III. RESULTS

A. Precision validation

To validate the effectiveness of the PID controller iteration downward continuation method, electromagnetic responses on the ground and in the air are calculated based on a uniform half-space model when the conductivity is equal to 0.01 S/m. The distance between the survey points is 10 m. The survey points are selected randomly, which are at x = 0 m, y = 150 m; x = 0 m, y = 200 m; x = 150 m, y = 200 m; and x = 200 m, y = 200 m. The PID controller iteration parameters are k_p = 4, k_d = 0.9 and k_i = 0.3. The downward continuation results are shown in Fig. 5. The black line is the electromagnetic response for h = 30 m. The red dotted line is analytical solution on the ground. The blue line is electromagnetic response after downward continuation. The Fig. 5 shows that downward continuation results are coincide with analytical solution. The average relative error of all the survey points is only 0.08%.

B. Interpretation results

1) Theoretical model

To verify the interpretation results of the downward continuation data, an example of a quasi-two-dimensional three-layer geology model was designed and is shown in Fig. 6 (a) and Fig. 7 (a). The calculation parameters are as follows: the start point of the grounded electrical transmitter is x = -500 m, y = 0 m, and the end point is x = 500 m, y = 0 m on the ground. The transmitter current is I = 10 A, the induction coil equivalent area is S = 10000 m^2, and the receiver locations are x = 20 m - 100 m, y = 500 m and z = 30 m. The model parameters of Fig. 6 (a) are as follows: the bedrock has 200 Ω·m electrical resistivity, and the low-resistivity layer is recorded at 20 Ω·m, whose depth varies from -60 m to -80 m. The model parameters of Fig. 7 (a) are as follows: The depth of the low-resistivity layer varies from -160 m to -180 m. The other model parameters are the same as Fig. 6 (a). The z = 30 m electromagnetic responses are calculated, and then the responses are downward continuation to the ground. The continued electromagnetic response and z = 30 m electromagnetic response are interpreted by section interpretation method. The interpretation results are shown in Figs. 6 (b), (c) and Figs. 7 (b), (c).

Figures 6 (b) and 7 (b) are the interpretation results of the z = 30 m electromagnetic response, and Figs. 6 (c) and 7 (c) are the interpretation results of continued electromagnetic responses. For the shallow abnormality case, the results of the z = 30 m electromagnetic responses, as shown in Fig. 6 (b), indicate that the thickness is much greater than that of the results for continued electromagnetic responses, as shown in Fig. 6 (c). For the deep abnormality case, the results of the low resistivity abnormality are similar. But the shallow part of continued electromagnetic responses, as shown in Fig. 7 (c), is more similar to the true model than the results of the z = 30 m electromagnetic response, as shown in Fig. 7 (b). The results show that continued electromagnetic responses are nearly equivalent to the true model. The accuracy of data interpretations could be improved by the PID controller iteration downward continuation method.

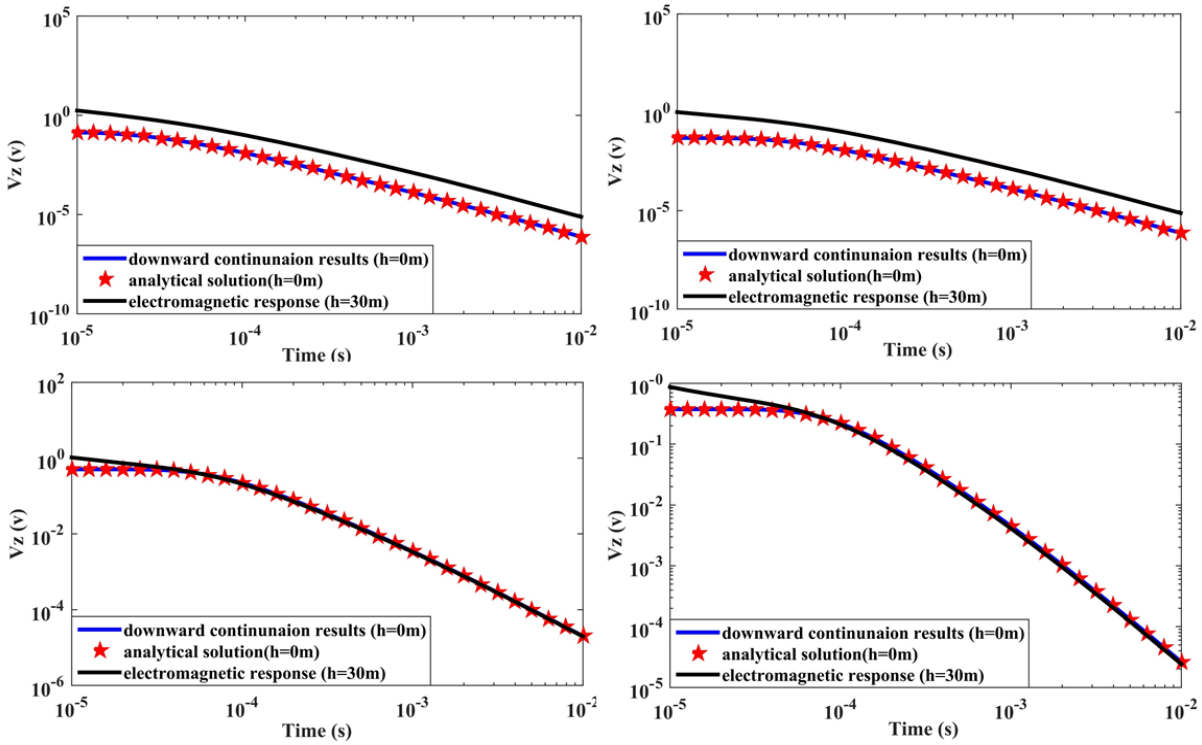

Fig. 5. Downward continuation results at different survey points: (a) x=0 m, y=150 m; (b) x=0 m, y=200 m; (c) x=150 m, y=200 m; (d) x=200 m, y=200 m.

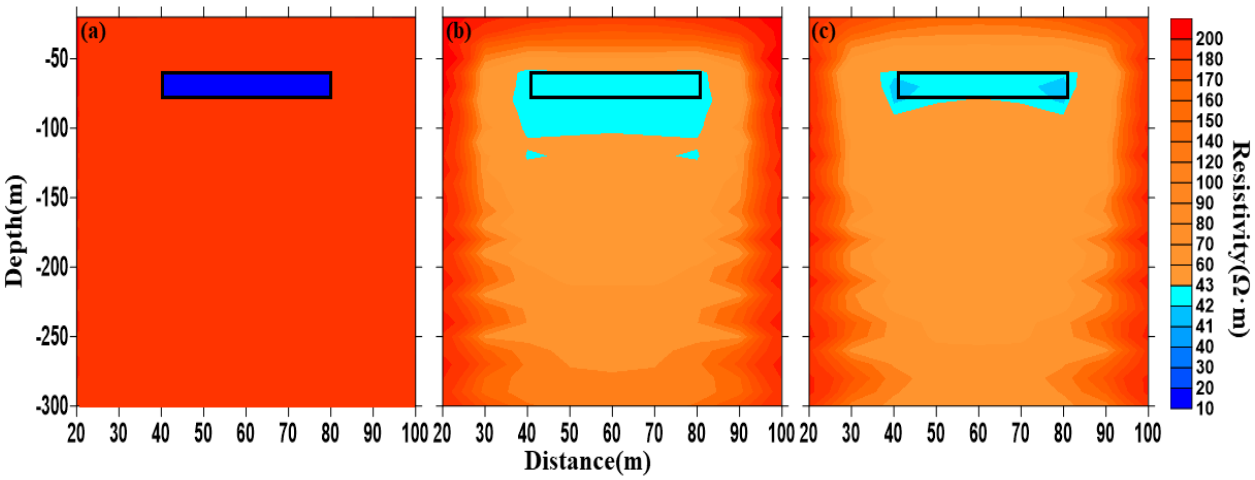

Fig. 6. Comparison between depth section images of the shallow abnormality: (a) theoretical model, (b) interpretation results derived from the z = 30 m electromagnetic response, and (c) interpretation results derived from continued electromagnetic responses. The black outlines serve as a reference to the theoretical model.

2) Field data results

To verify an effectiveness of the PID controller iteration downward continuation method, it is applied to field data. We conducted an exploration experiment at Shouyang, Jinzhong City, Shanxi Province, China, in2016 December by using a GATEM system. The field site is chosen because there is a borehole in the survey area. According to the Shanxi Geological Survey, the order of the geological structures from the top to the bottom is Quaternary strata, Permian system, Carboniferous system and Ordovician system. The Quaternary strata mainly consists of loess and clay, and the electrical resistivity is relatively low. The Permian system is composed of mudstone, sandstone, fine-

grained sandstone and coal seams, and the electrical resistivity is relatively high. It is the main coal-bearing stratum that can be exploited. The main constituents of the Carboniferous system are siltstone, mudstone, bauxite, limestone and coal seam. The Ordovician system is the basement of the coal seam, and the main lithology is dark gray layered limestone with high electrical resistivity. The survey area covers the known mined-out area. The electrical resistivity of this area is very low, and the surface depth is approximately 100 m. The mined-out area thickness is 20 m. The mined-out area and Permian system contain water; therefore, the electrical resistivity may be lower than itself, and the low-resistivity layer may be thicker than the mined-out area thickness.

The survey area and flight path are shown in Fig. 8. The electrical transmitting system used a grounded wire source with a length of 2 km. The transmitter current was 40 A, the frequency was 12.5 Hz, and the transmitter waveform was a bipolar square wave which was +40 A, 0 A, -40 A, 0 A. The induction coil area was 2,160 m^2, the sampling rate of receiver was 30 kHz, the receiver locations were x = 60 m - 1980 m, y = 300 m and the flight altitude was z = 30 m. The flight path was parallel to the grounded wire source.

Baseline correction is performed on field data by a method based on wavelet transform [26]. Decay curves are stacked 8 times to suppress random noise. To remove the electromagnetic signal noise, an exponential fitting-adaptive Kalman filter (EF-AKF) is used [12]. The denoised field data is continuation downward to the ground. The continued electromagnetic data, the results of raw data and the denoised z = 30 m field data are interpreted [10]. The depth section images are shown in Fig. 9.

Figure 9 (a) presents the interpretation results of raw data, Fig. 9 (b) presents the results of denoised z = 30 m field data, and Fig. 9 (c) presents the results of the continued electromagnetic data. The low resistivity layer under 200 m, in Fig. 9 (a), is the mined-out area with accumulated water, which is deeper than the true depth. The thickness of low resistivity layer is more than 100 m which is much thicker than its true thickness. The low resistivity layer at 100 m, in Figs. 9 (b) and (c), which are consistent with the survey area. In Fig. 9 (b), the results of denoised z = 30 m field data, the thickness of low resistivity layer is around 50 m. In Fig. 9 (c), the results for the continued electromagnetic data, the thickness of the low resistivity layer is average 36 m which is smaller than the results of denoised z = 30 m field data and closer to true thickness. The results show that the PID controller iteration downward continuation method can be effectively applied to the denoised field data and it can approve the interpretation accuracy of GATEM data.

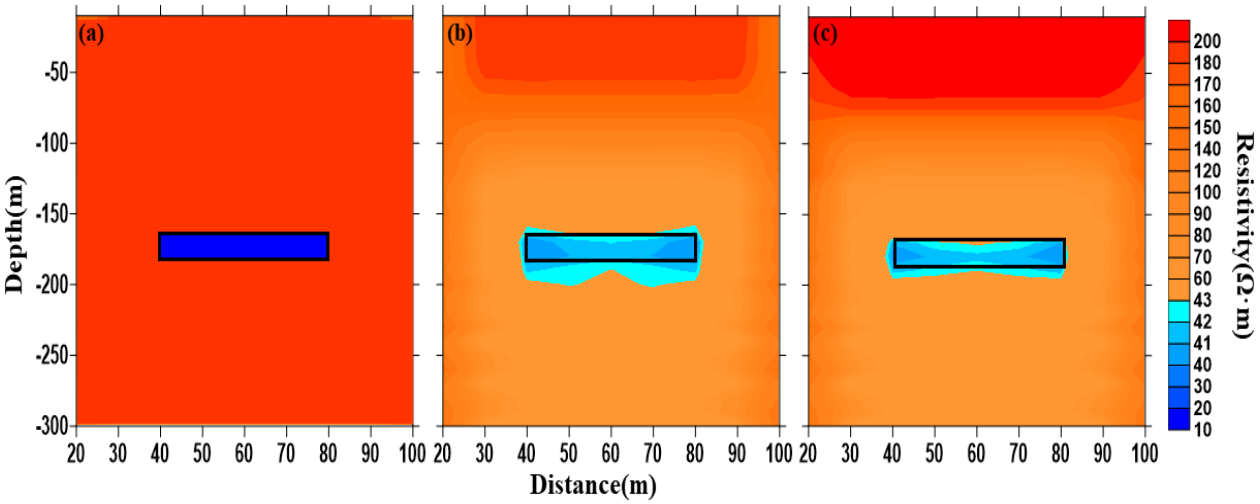

Fig. 7. Comparison between depth section images of the deep abnormality: (a) theoretical model, (b) interpretation results derived from the z = 30 m electromagnetic response, and (c) interpretation results derived from continued electromagnetic responses. The black outlines serve as a reference to the theoretical model.

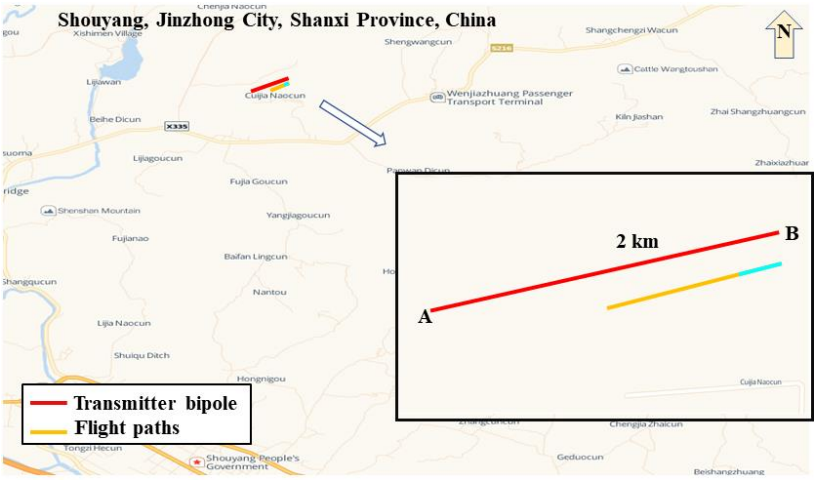

Fig. 8. Survey area for Shouyang, Jinzhong City, Shanxi Province in China. The red line is the transmitter line with 2 km length, and the electrical dipole A is 0. The yellow line is the flight path which is parallel to the red line. The blue line is the chosen section for verifying the application of the downward continuation.

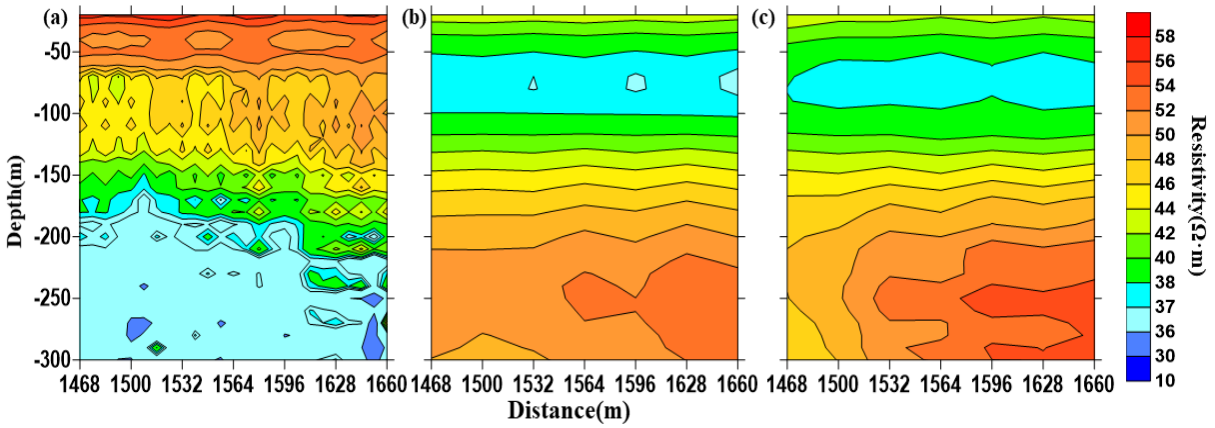

Fig. 9. Depth section images from the field data: (a) the results of raw data, (b) the results of the z = 30 m field data, and (c) the interpretation results of the continued electromagnetic continuation.

IV. CONCLUSION

The GATEM system is an effective method for the exploration of low resistivity anomalies in complex areas. In this paper, a PID controller iteration downward continuation method is proposed to improve the interpretation and imaging accuracy of GATEM data. The integral and differential term are added into the traditional iterative method. Compared with the analytical solution, the continuation downward accuracy of the iterative method is verified, and the iteration time is effectively reduced. This method is validated using synthetic data interpretation and is compared with the interpretation results of the z = 30 m electromagnetic response. The results show that interpretation of continued electromagnetic response is more consistent with the true model, especially for the shallow anomalous body. To further verify the effectiveness, this method is applied to field data of Shouyang, Yangquan City, Shanxi Province, China, which improves the quality of the GATEM field data results. This method has significant implications for the GATEM exploration.

ACKNOWLEDGMENT

This study was carried out within the framework of the project ‘3D Numerical Simulation of ATEM Based on Conformal Mesh Technique (JJKH20190127KJ)’ supported by the Planning Project of Science and Technology and Humanities and Social Science Research of the Education Department of Jilin Province and the project ‘Research on Sub-diffusion Multi-parameter extraction method of Ground-source Airborne Electromagnetic data based on fully connected neural network (42004059)’ and ‘Research on Key Technologies of Electromagnetic Detection of Induction-Polarization

Symbiosis Effects of Dual Phase Conductive Medium Based on SQUID technique (42030104)' supported by the National Natural Science Foundation of China.

REFERENCES

[1] T. Mogi, K. Kusunoki, H. Kaieda, H. Ito, A. Jomori, N. Jomori, and Y. Yuuki, "Grounded electrical-source airborne transient electromagnetic (GREATEM) survey of Mount Bandai," *North-Eastern Japan, Exploration Geophysics*, vol. 40, no. 1, pp. 1-7, Feb. 2009.

[2] H. Ito, H. Kaieda, T. Mogi, A. Jomori, and Y. Yuuki, "Grounded electrical-source airborne transient electromagnetics (GREATEM) survey of Aso volcano," *Japan. Explor. Geophys*., vol. 45, pp. 43-48, Mar. 2014.

[3] M. J. Yi, J. H. Kim, N. H. Sung, M. H. Han, K. Motschka, R. Supper, A. Ahl, and A. Johmori, "Test airborne EM surveys at a black-shale type uranium deposit in Korea," *Near Surface Geoscience 2016 - 22nd European Meeting of Environmental and Engineering Geophysics*, Sep. 2016.

[4] D. Li, Z. Tian, Y. Ma, J. Gu, Y. Ji, and S. Li, "Application of grounded electrical source airborne transient electromagnetic (GREATEM) system in goaf water detection," *Journal of Environmental & Engineering Geophysics*, vol. 24, no. 3, pp. 387-397, Sep. 2019.

[5] Y. Sasaki, M. J. Yi, J. Choi, and J. S. Son, "Frequency and time domain three-dimensional inversion of electromagnetic data for a grounded-wire source," *Journal of Applied Geophysics*, vol. 112, pp. 106-114, Jan. 2015.

[6] S. A. Allah and T. Mogi, "Three-dimensional resistivity modeling of GREATEM survey data from ontake volcano," *Northwest Japan [J]. Earth Planets & Space*, vol. 68, no. 1, pp. 76, Dec. 2016.

[7] B. Liang, C. Qiu, F. Han, C. Zhu, N. Liu, H. Liu, F. Liu, G. Fang, and Q. H. Liu, "A new inversion method based on distorted born iterative method for grounded electrical source airborne transient electromagnetics," *IEEE Transactions on Geoscience and Remote Sensing*, vol. 56, no. 2, pp. 877-887, Mar. 2018.

[8] Q. Wu, D. S. Li, C. D. Jiang, Y. J. Ji,Y. L. Wen, and H. Luan, "Ground-source airborne time-domain electromagnetic (GATEM) modelling and interpretation method for a rough medium based on fractional diffusion," *Geophysical Journal International*, vol. 217, no. 3, pp. 1915-1928, June 2019.

[9] T. Mogi, Y. Tanaka, K. Kusunoki, T. Morikawa, and N. Jomori, "Development of grounded electrical source airborne transient EM (GREATEM)," *Exploration Geophysics*, vol. 29, pp. 61-64, June 1998.

[10] Y. Ji, G. Yang, and S. Guan, "Interpretation research on electrical source of time domain ground - Airborne electromagnetic data," *2011 International Conference on Green Environmental Sustainable Development*, Jan. 2011.

[11] D. Li, Y. Wang, J. Lin, S. Yu, and Y. Ji, "Electromagnetic noise reduction in grounded electrical-source airborne transient electromagnetic signal using a stationary wavelet-based denoising algorithm," *Near Surface Geophysics*, vol. 15, no. 2, pp. 163-173, Apr. 2017.

[12] Y. Ji, Q. Wu, Y. Wang, J. Lin, D. Li, S. Du, S. Yu, and S. Guan, "Noise reduction of grounded electrical source airborne transient electromagnetic data using an exponential fitting-adaptive Kalman filter," *Exploration Geophysics*, vol. 49, no. 3, pp. 243-252, Mar. 2017.

[13] M. Fedi and G. Florio, "A stable downward continuation by using the ISVD method," *Geophysics Journal International*, vol. 151, pp. 146-156, Apr. 2002.

[14] S. Xu, "A comparison of effects between the iteration method and FFT for downward continuation of potential fields," *Chinese Journal of Geophysics*, vol. 50, no. 1, pp. 285-289, Jan. 2007.

[15] S. Xu and H. Yu, "The interpolation-iteration method for potential field continuation from undulating surface to plane," *Acta Geophysica Sinica*, vol. 50, no. 6, pp. 1811-1815, Nov. 2007.

[16] A. E. Ali, Z. Liu, Y. Bai, A. G. Farwa, A. S. Ahmed, and G. Peng, "A stable gravity downward continuation for structural delineation in Sulu Sea region," *Journal of Applied Geophysics*, vol. 155, pp. 26-35, Aug. 2018.

[17] C. Zhang, Q. Lv, J. Yan, and G. Qi, "Numerical solutions of the mean-value theorem: New methods for downward continuation of potential fields," *Geophysical Research Letters*, pp. 3461-3470, Apr. 2018.

[18] G. R. J. Cooper, "The downward continuation of the tilt-angle," *Near Surface Geophysics*, vol. 14, no. 5, pp. 385-390, Oct. 2016.

[19] G. R. J. Cooper, "The downward continuation of aeromagnetic data from magnetic source ensembles," *Near Surface Geophysics*, vol. 17, pp. 101-107, Apr. 2019.

[20] M. Nabighian, "Electromagnetic methods in applied geophysics," *Society of Exploration Geophysicists*, vol. 1, pp. 528, Jan. 1988.

[21] D. Guptasarma and B. Singh, "New digital linear filters for Hankel J0 and J1 transforms," *Geophysical Prospecting*, vol. 45, pp. 745-762, Oct. 1997.

[22] D. Guptasarma, "Optimization of short digital linear filters for increased accuracy," *Geophysical*

Prospecting, vol. 30, pp. 501-514, Aug. 1982.
[23] M. Nabighian, "Foreword and introduction," *Geophsics*, vol. 49, pp. 849-853, July 1984.
[24] A. B. Rad and W. L. LO, "Predictive PI controller," *International Journal of Control*, vol. 60, no. 5, pp. 953-975, Nov. 1994.
[25] B. R. Spies, "Depth of investigation in electromagnetic sounding methods," *Geophysics*, vol. 54, no. 7, pp. 872-888, July 1989.
[26] Y. Wang, Y. Ji, S. Li, J. Lin, F. Zhou, and G. Yang, "A wavelet-based baseline drift correction method for grounded electrical source airborne transient electromagnetic signals," *Explor. Geophys*, vol. 44, pp. 229-237, Dec. 2013.

Shanshan Guan received the Ph.D. degree in Measuring and Testing Technology and Instrument from Jilin University, Changchun, China, in 2012. In 2019, she was a Visiting Scholar with the Southern University of Science and Technology, China. Since 2012, she has been with the College of Instrumentation and Electrical Engineering, Jilin University, where she is currently an Associate Professor. Her research interests include the development of transient electromagnetic instruments and data forward, and inverse algorithms.

Qiong Wu received the B.S. degree in Electrical Engineering and Automation from Jilin Unversity, Changchun, China, in 2013 and the Ph.D. degree in Detection Technology and Automatic Equipment from Jilin Unversity, Changchun, China, in 2019. From 2016 to 2017, she was an exchange student in Sustainable Resources Engineering, Faculty of Engineering, Hokkaido University, Sapporo, Japan. Her research interest includes modelling and interpretation method for grounded electrical source airborne electromagnetics.